

# Research Activities on Numerical and Experimental Studies of Cavitation Instabilities in the Rocket Engine Turbopump

Keita Yamamoto<sup>1†</sup>, Satoshi Ukai<sup>1</sup>, Mitsuru Shimagaki<sup>2</sup>, Satoshi Kawasaki<sup>2</sup>, and Hideyo Negishi<sup>1</sup>

<sup>1</sup>Research Unit III, R&D Directorate, JAXA  
Tsukuba, Ibaraki, Japan

<sup>2</sup>Research Unit IV, R&D Directorate, JAXA  
Kakuda, Miyagi, Japan

yamamoto.keita@jaxa.jp

<sup>†</sup>Corresponding author

## Abstract

The present article demonstrates the recent research activities conducted in JAXA for turbopump inducers, focusing on flow characterizations by PIV measurements and establishment of cavitation surge prediction model. The PIV measurements successfully characterize the backflow structures in inducers. Especially, backflow vortices are captured by PIV from upstream views with a borescope. Furthermore, the study establishes a new prediction model for cavitation surge based on cavitation characteristic parameters. By integrating their dynamic properties, the model successfully predicts both frequency and onset of cavitation surge. The investigations will be further deepened to expand the insight of flow dynamics in inducers.

## 1. Introduction

For a mission of reusable rockets, modern rocket engines are demanded to achieve a flexible control of output power in the course of complex operational sequences, such as controlled reentry and landing. This in turn requires versatile abilities of turbopumps with an adjustable range of operations. However, the extension of turbopumps' operating range may increase a risk of cavitation development in an inducer situated upstream of a main pump, and cavitation can be a source of large pressure fluctuations and structural vibrations. In particular, flow instabilities caused by the cavitation development (so-called cavitation instabilities) are ones of the most damaging phenomena in turbopumps, often leading to a mission failure. For example, an accident of the Japanese launch vehicle (H-II rocket No.8) in 1999 is assumed to be attributed to one of the cavitation instabilities, rotating cavitation (see Fig.1<sup>1</sup>). Since then, characteristics of cavitation instabilities were extensively studied in experiments<sup>2-4</sup> and simulations.<sup>5-7</sup>

Inducers are generally operated with a negative flow incidence at the blade inlet, which leads to a formation of backflow at the inlet. The backflow structure generally causes a development of blade tip cavitation and backflow vortex cavitation,<sup>8</sup> of which the dynamic features are considered to closely link with the cavitation instabilities observed in inducers. To obtain a better understanding of these backflow structures, the flow characteristics in inducers

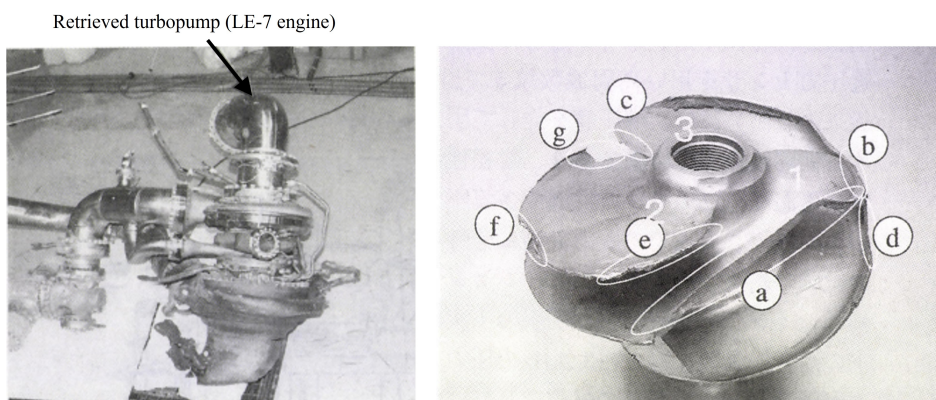


Figure 1: Recovered turbopump of LE-7 engine in H-II No.8 and damaged inducer<sup>1</sup>

## SHORT PAPER TITLE

were experimentally investigated by measurements,<sup>9,10</sup> visualizations,<sup>11</sup> and numerical simulations.<sup>12</sup> In the aspect of cavitation instabilities' evaluations, cavitation characteristic parameters in inducers (called cavitation compliance and mass flow gain factor) were introduced,<sup>13</sup> and often combined with one-dimensional model applications to predict features of cavitation instabilities.<sup>14-16</sup> The characteristics of these cavitation parameters were also investigated by experiments<sup>17-19</sup> and numerical simulations.<sup>20</sup>

Despite a number of studies about cavitation instabilities in inducers, an accurate prediction of cavitation instabilities still remains a challenge due to the missing link between flow dynamics and cavitation characteristics arising from the complex nature of cavitating flow. To fill this gap, the authors have performed researches to comprehend dynamics of flow and cavitation in inducers from both aspects of experiments and numerical simulations. The present article introduces research activities recently conducted in JAXA, focusing on the flow characterization by PIV measurements and the establishment of the prediction model for cavitation surge by characteristic parameters.

## 2. Cavitation instabilities in inducers

The cavitation development in inducers often causes flow instabilities in turbopumps and feedline systems. In particular, the following two phenomena are ones of the most harmful instabilities to be avoided for rocket engine operations.

- Rotating cavitation
- Cavitation surge

Rotating cavitation is a phenomenon in which an unequivalent length of the cavitation on each inducer blade periodically fluctuates (see Fig.2(a)), which appears that the unequivalent cavitation on the blade propagates in the rotating/counter-rotating direction from the view of the inducer (so-called rotating fluctuation mode). The propagation of the cavitation induces high frequency oscillations of pressure and stress on the blade. The stress oscillation gives a fatigue damage to the inducer blades, and leads to fatigue failure in the worst case as seen in Fig.1.

Cavitation surge is a phenomena where an entire cavitation volume on all the inducer blades is synchronously fluctuated (so-called axial fluctuation mode, see Fig.2(b)). The image duration approximately corresponds to one cycle of cavitation surge). Cavitation surge induces flow rate fluctuations in feedline systems, which is especially amplified in case that the oscillational frequency coincides with one of the structural eigenfrequencies of the rocket systems (called POGO instability<sup>21</sup>).

To accurately evaluate the features of these critical cavitation phenomena in turbopumps, better comprehensions of fundamental physics behind flow features and cavitation dynamics in inducers are of key importance. In the following sections, two research activities recently conducted to expand our insight of flow instabilities in inducers are presented.

(a) Visualization of rotating cavitation (every one inducer rotation)



(b) Visualization of cavitation surge (every one inducer rotation)

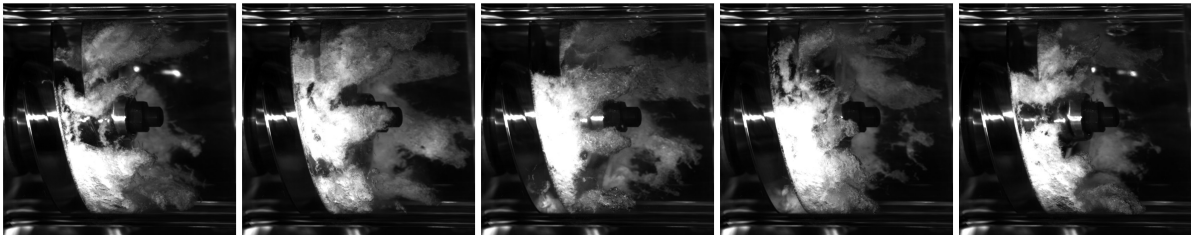


Figure 2: High-speed visualizations of rotating cavitation and cavitation surge taken at JAXA Kakuda space center (images every one inducer rotation, looking at the same blade)

### 3. Flow characterization of inducer by PIV measurement

As mentioned earlier, backflow structures and associated vortices developed in inducers appear to have an essential link with a flow instabilities. In the past, one of the authors performed the velocity measurement by PIV (Particle Image Velocimetry) to obtain a fundamental characteristics of flow field in an inducer.<sup>10,22</sup> In recent years, the authors extended the measurement to a high-frequency PIV, as well as the one using a borescope that allows an optical view from the upstream side of the inducer. These PIV measurements are conducted in the closed-loop water tunnel installed in JAXA Kakuda space center (see Fig.3(a) for test facility's schematics). In Fig.3(b), an example of the PIV measurement setup in the experiment is presented. The detailed systems for the performed PIV measurements are summarized in Tab.1.

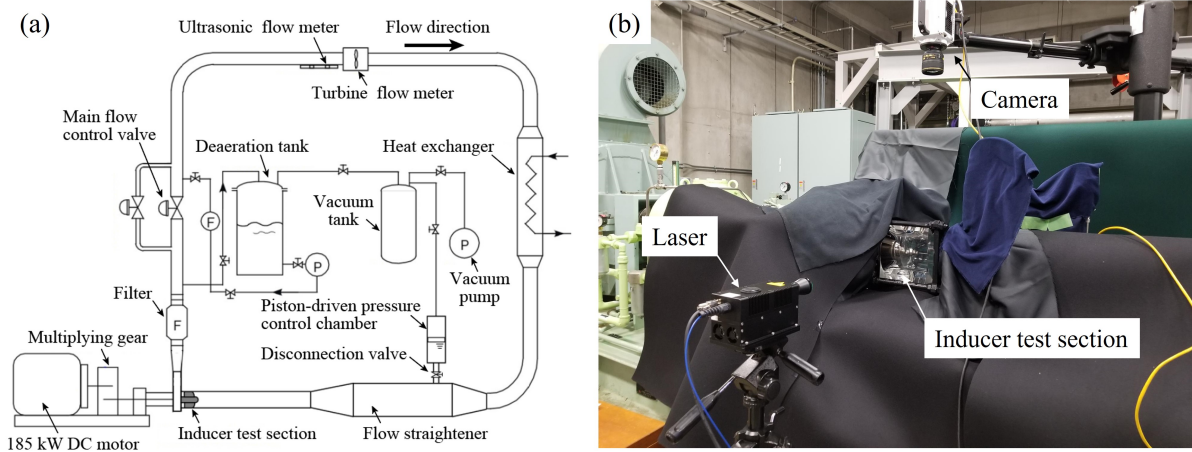


Figure 3: Schematics of the experimental facility at JAXA Kakuda Space Center (a) and the example of PIV measurement setup (b)

Table 1: Details of setup for PIV measurements

	<b>PIV on axial plane</b>	<b>PIV on tangential plane</b>
Laser	CW Laser (Continuous emission laser)	Double-pulsed Nd:YAG laser
Camera	Phantom T1340	Phantom T1340
Optics	Nikkor 85mm f1.8	Nikkor 135mm f2.0 + borescope
Acquisition frequency	6,000 Hz	10 Hz

In Fig4, the distributions of the averaged axial velocity and the RMS of the velocity obtained from the PIV measurements on the axial plane for  $Q/Q_d = 1.0, 0.9,$  and  $0.8$  are presented. It can be seen that the backflow region is clearly enlarged with respect to the decrease of flow rate. Furthermore, the RMS of the velocity magnitude is remarkably increased at the interface between the backflow and forward flow regions, and the high RMS region is enlarged as a decrease of the flow rate. It is assumed that the high value of RMS in this region is attributed to backflow vortices formed by the shear layer, which is induced by the backflow having the circumferential velocity component and the main flow without the circumferential velocity component.

In Fig.5, the averaged velocity field on the tangential plane upstream of the inducer obtained by the PIV measurements with a borescope for  $Q/Q_d = 1.0, 0.9,$  and  $0.8$  are presented. The location of the measurement plane is illustrated as a dashed line in Fig.4. It is clarified that the strong circumferential velocity field is observed in the backflow region near the casing wall at  $Q/Q_d = 0.9$  and  $0.8$ , whereas no circumferential velocity component nearly exists at  $Q/Q_d = 1.0$  since the backflow region does not reach the measurement section (see Fig.4). Furthermore, the magnitude of the tangential flow velocity in the backflow region is increased when the flow rate is decreased, suggesting that the development of backflow vortices may be also intensified.

In Fig.6, the comparison of the instantaneous vorticity distributions on the tangential plane for  $Q/Q_d = 1.0, 0.9,$  and  $0.8$  together with the instantaneous velocity vector is presented. Particularly for  $Q/Q_d = 0.9$  and  $0.8$ , the high vorticity regions caused by backflow vortices appear in the interface between the backflow region with high circumferential velocity and the main flow. Since the PIV measurement on the tangential plane with borescope was performed

## SHORT PAPER TITLE

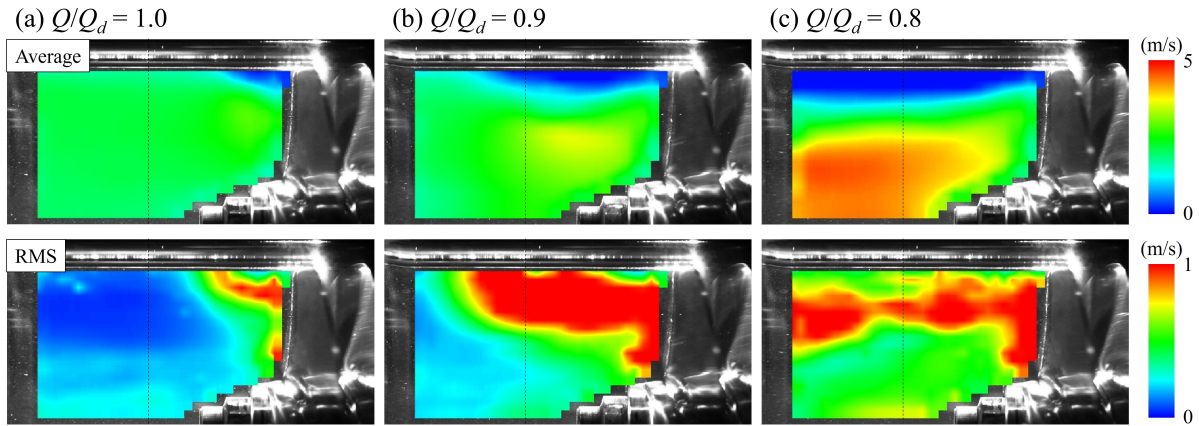


Figure 4: Comparisons of averaged axial velocity and RMS obtained from PIV measurements on axial plane for different flow rate conditions

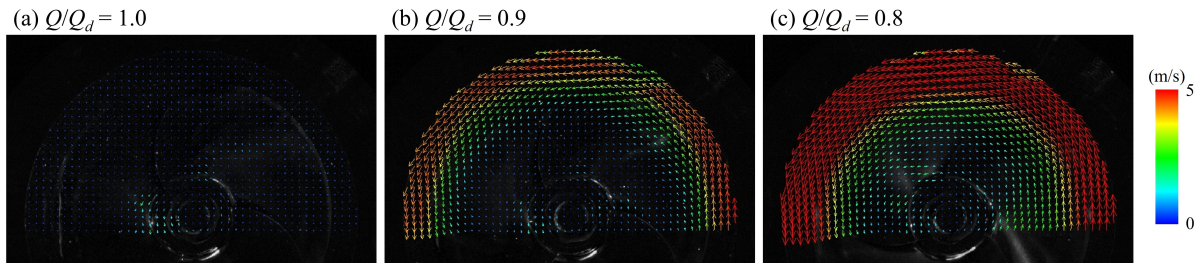


Figure 5: Comparisons of the averaged velocity obtained from PIV measurements on tangential plane with borescope for different flow rate conditions

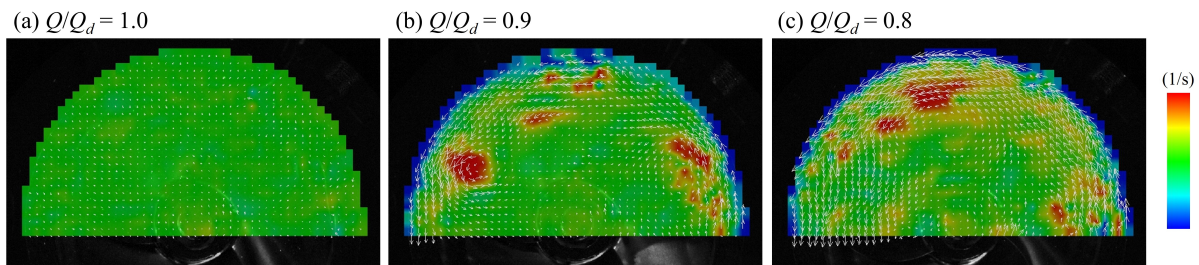


Figure 6: Instantaneous vorticity distributions on tangential plane for different flow rate conditions

on the half of the section with the time resolution 10 Hz, the number of backflow vortices as well as their progressing frequency cannot be characterized. Nonetheless, it is worth mentioning that the vortical structures in this measurement section consistently appear at almost every timestep especially for  $Q/Q_d = 0.9$ , which suggests that the intensities of the circumferential velocity component in the backflow region may be a key factor to develop backflow vortices.

In Fig.7, the time history of the axial and radial ( $x$  and  $y$ ) velocity components and its frequency analysis result (PSD, power spectrum density) at three locations acquired by the PIV measurement on the axial plane for  $Q/Q_d = 0.9$  with the time resolution 6000 Hz is presented. At Position A located near the boundary of the backflow region, the velocity components are clearly oscillated periodically. In the frequency analysis result, the peaks appear at  $f/f_n = 0.47$  and  $0.66$  ( $f_n$ : inducer rotational frequency). Based on the observation of vorticities at the tangential plane, the number of backflow vortices is assumed to be 3 or 4. If assuming that the number of vortices is 3, the precession frequency of the backflow vortices is roughly estimated as  $0.15 \times f_n$ , which is consistent with the past experimental results.<sup>9,12</sup> These frequency peaks are, in contrast, reduced at Position B and C (the dominant peak appears at the blade passing frequency  $f/f_n = 3$  at Position B, and almost no dominant peaks are found at Position C). The dynamic characteristics of backflow vortices, especially the number of vortices and their precession frequency, will be furthermore investigated in the future by applying high-speed PIV to the tangential plane.

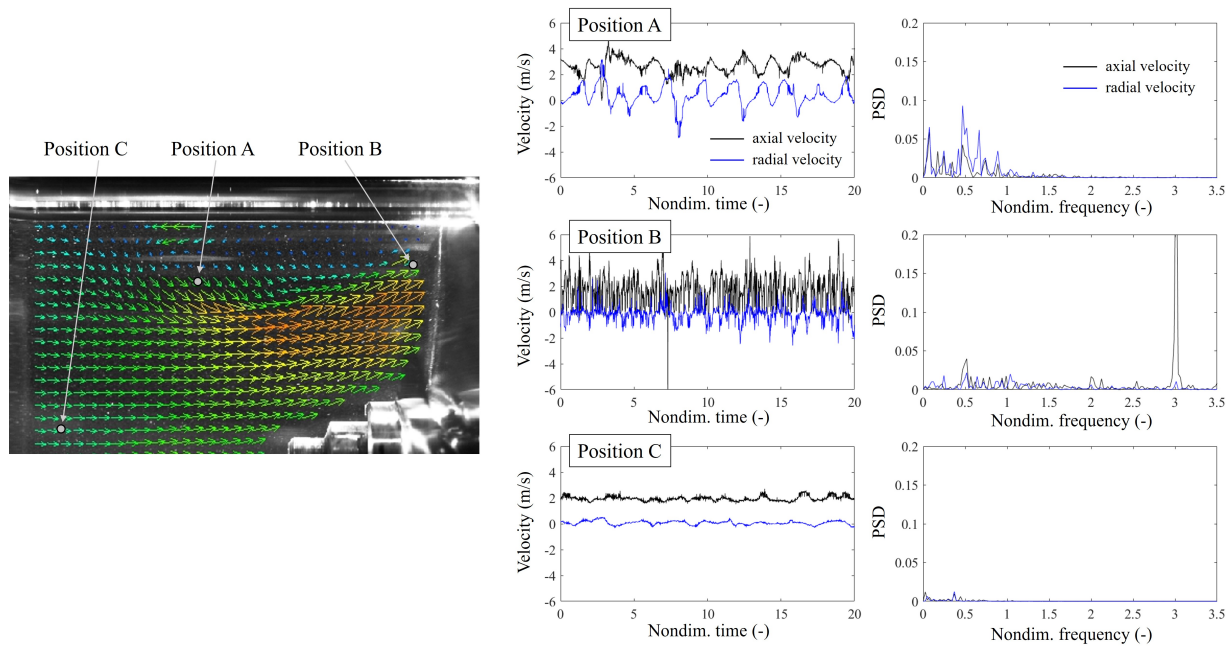


Figure 7: Time history and frequency analysis result of axial and radial velocity components obtained by high-speed PIV measurements on axial plane at  $Q/Q_d = 0.9$

#### 4. Establishment of cavitation surge prediction model

In order to evaluate risks of the cavitation instabilities' occurrence at an early phase of designing turbomachinery, it is required to predict cavitation instabilities by a plane model. In the past years, a number of researchers discussed prediction models based on one-dimensional approach by introducing cavitation characteristic parameters, called cavitation compliance and mass flow gain factor.<sup>8,14,16</sup> However, none has achieved quantitative and practical predictions of cavitation instabilities by a parametric model thus far. The authors recently suggested a new parametric model to enable predictions of cavitation surge onset and frequency more accurately based on the characteristic parameters of cavitation by integrating their dynamic properties.<sup>23</sup>

The characteristic parameters of cavitation, cavitation compliance  $K$  and mass flow gain factor  $M$ , are respectively defined by the derivatives of cavitation volume in the inducer  $V$  by pressure  $p$  and flow rate  $Q$  ( $K = \partial V / \partial p$  and  $M = \partial V / \partial Q$ ). These parameters are first evaluated by a series of steady RANS calculations conducted with periodic single-passage domain. (see Fig.8, the details of the simulation are also summarized) In Fig.9(a), the comparison of simulated cavitation region (highlighted by iso-surface of void fraction 0.1) with the visualized cavitation in the experiment for different cavitation number  $\sigma (= 2(p_{in} - p_v) / \rho U_t^2)$ ,  $p_{in}$ : inducer inlet pressure,  $p_v$ : vapor pressure,  $U_t$ : inducer tip velocity) are presented. It is confirmed that the cavitation region in the inducer is appropriately captured by the performed simulation. In Fig.9(b), the values of cavitation compliance  $K$  and mass flow gain factor  $M$  computed from the conducted simulations are presented together with the past measurement results in different inducers. It can be observed that the evaluated parameters have the same tendency as the past experimental results, suggesting that the characteristic parameters are well evaluated by the conducted simulations.

The parametric model to estimate the cavitation surge features is developed by the one-dimensional approach.

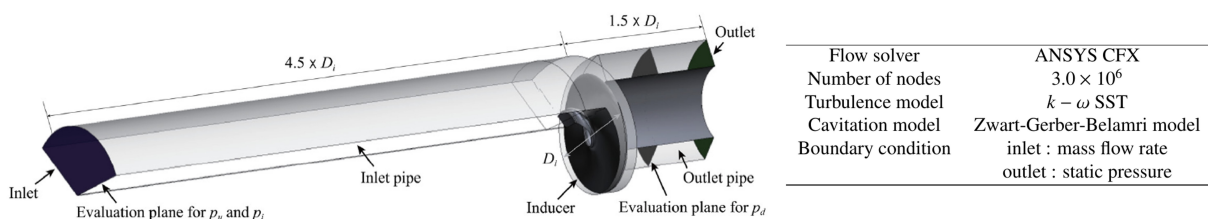


Figure 8: Adopted computational domain and simulation setup

## SHORT PAPER TITLE

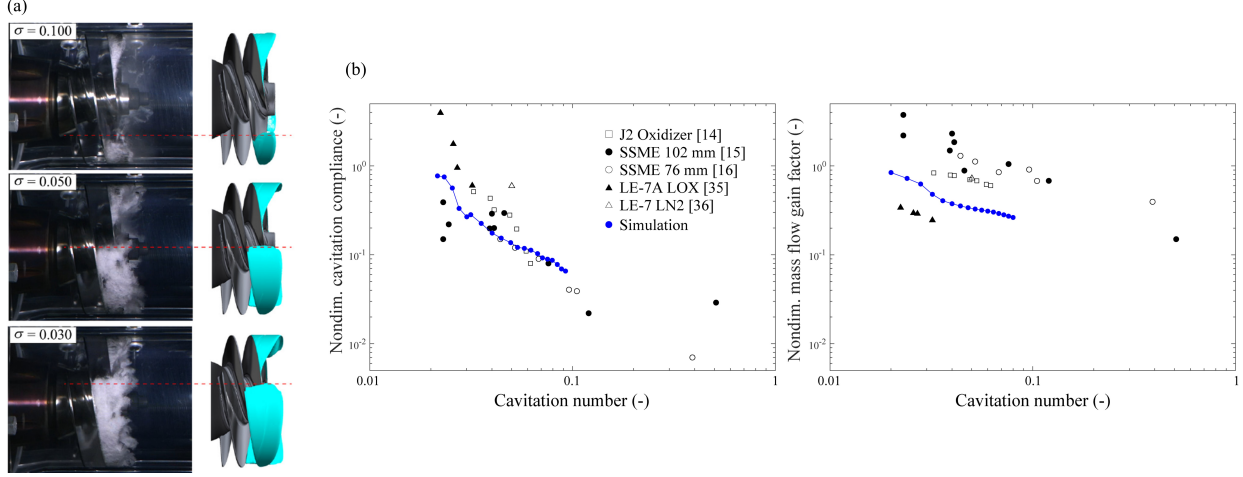


Figure 9: Comparisons of simulated cavitation region (a), evaluated cavitation compliance and mass flow gain factor (b)

By applying the one-dimensional unsteady Bernoulli equation and continuity equation to the inducer test facility in Kakuda space center, the following differential equation regarding the flow rate can be obtained.

$$\frac{\partial^2 \bar{Q}}{\partial t^2} + \left( -\frac{A_i}{\rho L} \frac{M}{K} + \frac{\bar{Q}}{A_i L} D + \frac{\bar{Q}}{A_i L} R \right) \frac{\partial \bar{Q}}{\partial t} + \left( \frac{A_i}{\rho L K} + \frac{A_i}{\rho L C_a} \right) \bar{Q} = 0 \quad (1)$$

where  $A_i$  is the inlet area of the inducer,  $L$  is the length between inducer and accumulator,  $D$  is the diffusion factor,  $R$  is the resistance coefficient,  $C_a$  is the compliance in the accumulator, and  $\sim$  and  $-$  indicate fluctuating and mean values, respectively. The further improvement of the model is proposed by integrating dynamic characteristics of cavitation compliance and mass flow gain factor expressed by complex quantities such as  $K' = K e^{j\beta_K}$  and  $M' = M e^{j\beta_M}$  where  $\beta_K$  and  $\beta_M$  are the phase properties varied depending on the frequency. By assuming the same phase delay of  $K$  and  $M$ , the onset condition and the frequency of cavitation surge obtained from eq.1 are then written as the following equation (eq.2 for the onset condition and eq.3 for the frequency of cavitation surge, see more details in<sup>23</sup>).

$$\zeta = 2\phi K^*(D + R) - \frac{N}{2\pi\omega^*} \sin\beta_K - M^* \cos(\beta_M - \beta_K) < 0 \quad (2)$$

$$M^* \cos(\beta_M - \beta_K) > 2\phi K^*(D + R) - \frac{N}{2\pi\omega^*} \sin\beta_K$$

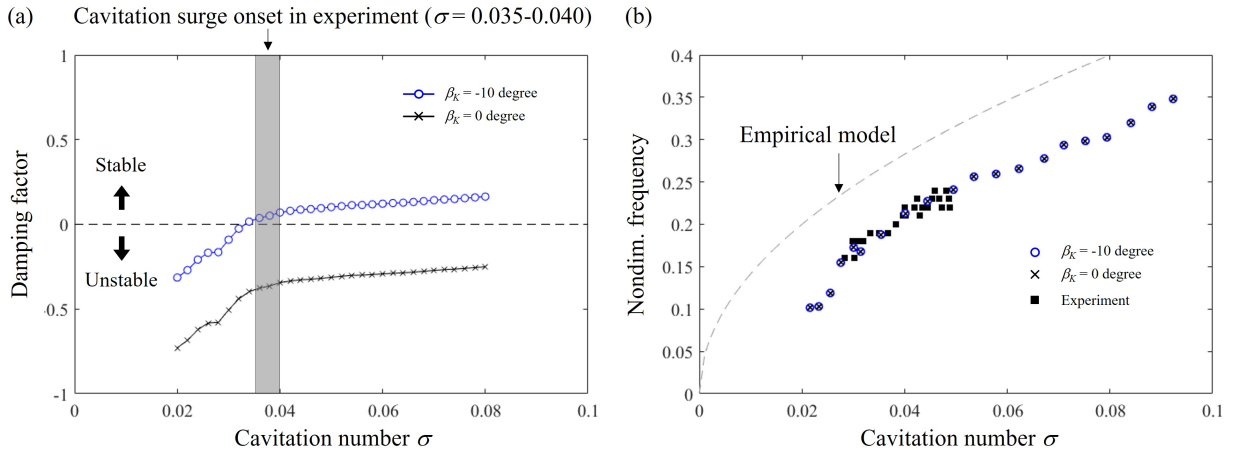


Figure 10: Prediction results of cavitation surge onset (a) and frequency (b) by proposed one-dimensional model

$$f_{cs} \approx \frac{1}{2\pi} \sqrt{\frac{A_i \cos \beta_K}{\rho L K}} \quad (3)$$

Note that  $K^*$  and  $M^*$  are the non-dimensional values of  $K$  and  $M$ . These equations clearly indicate that the phase properties of cavitation compliance are of key importance, especially for prediction of cavitation surge onset. Although the phase properties cannot be evaluated by the present method, it was shown that the value of  $\beta$  is approximately varied between 0 and -20 degree based on the past literature.<sup>18,19,24</sup> In Fig.10, the comparisons of cavitation surge onset and frequency with the experimental results are presented presuming the phase value of  $\beta_K = -10$  degree and  $\beta_K = 0$  degree (without phase delay). It can be observed that both frequency and onset conditions are well evaluated by the proposed model. Especially, the onset condition is adequately estimated by considering phase characteristics, whereas the prediction without phase ( $\beta_K = 0$ ) obviously fails to predict the onset. It should be mentioned that the accuracy of predicting the cavitation surge onset is improved by considering phase properties, while the frequency of cavitation surge is not largely affected by the phase. The authors continuously attempt to reveal the dynamic characteristics underlying cavitation in inducers to further improve the accuracy of the prediction for cavitation instabilities by parametric model to enable its application to design reliable turbopumps.

## 5. Conclusion

In the present study, the resent research activities for a turbopump inducer, focusing on PIV measurements and model estimation, are introduced, and the following remarks are obtained.

- PIV measurement with a borescope are successfully applied to capture the backflow vortices formed upstream of the inducer particularly at the low flow rate conditions. It is observed by the high-frequency PIV on the axial plane that the velocity at the interface between the backflow and forward flow regions have several fluctuation frequencies, which may relate to features of backflow vortices.
- Prediction models of cavitation surge are established based on the one-dimensional approach including dynamic characteristics of cavitation compliance  $K$  and mass flow gain factor  $M$ , and cavitation surge onset and frequency were evaluated by  $K$  and  $M$  obtained from the numerical simulations. As a result of comparisons with experimental results, both onset and frequency are adequately estimated, and especially the prediction accuracy of cavitation surge onset is improved by introduction of dynamic characteristics.

The researches presented above are on-going activities, and more investigations will be performed to achieve further comprehensions of flow dynamics in inducers.

## References

- [1] Konno Akira and Sakadume Norio. LE-7 engine turbopump and accident cause of H-II No.8 (in Japanese). *Turbomachinery*, 2001.
- [2] Angelo Cervone, Renzo Testa, Cristina Bramanti, Emilio Rapposelli, and Luca D'Agostino. Thermal effects on cavitation instabilities in helical inducers. *Journal of Propulsion and Power*, 21(5):893–899, 2005.
- [3] Junho Kim and Seung Jin Song. Visualization of rotating cavitation oscillation mechanism in a turbopump inducer. *Journal of Fluids Engineering, Transactions of the ASME*, 141(9), 2019. 091103.
- [4] Ruzbeh Hadavandi, Giovanni Pace, Dario Valentini, Angelo Pasini, and Luca D'Agostino. Identification of Cavitation Instabilities on a Three-Bladed Inducer by Means of Strain Gages. *Journal of Fluids Engineering, Transactions of the ASME*, 142(2), 2020. 021210.
- [5] Olivier Coutier-Delgosha, Yannick Courtot, Florence Joussellin, and Jean-Luc Reboud. Numerical Simulation of the Unsteady Cavitation Behavior of an Inducer Blade Cascade. *AIAA Journal*, 42(3):560–569, 2004.
- [6] Ashvin Hosangadi, Vineet Ahuja, and Ronald Ungewitter. Simulations of Rotational Cavitation Instabilities in the SSME LPFP Inducer. *43rd AIAA/ASME/SAE/ASEE Joint Propulsion Conference & Exhibit*, (AIAA-2007-5536), 2007.

## SHORT PAPER TITLE

- [7] Naoki Tani, Nobuhiro Yamanishi, and Yoshinobu Tsujimoto. Influence of flow coefficient and flow structure on rotational cavitation in inducer. *Journal of Fluids Engineering, Transactions of the ASME*, 134(2), 2012. 021302.
- [8] C Brennen. Hydrodynamics of Pumps. *Cambridge University Press*, 1994.
- [9] Yoshinobu Tsujimoto, Hironori Horiguchi, and Xiangyu Qiao. Backflow from inducer and its dynamics. *Proceedings of 2005 ASME Fluids Engineering Division Summer Meeting, FEDSM2005*, 2005:1678–1689, 2005.
- [10] Mitsuru Shimagaki, Tomoyuki Hashimoto, Mitsuo Watanabe, Satoshi Hasegawa, Yoshiki Yoshida, Toshiya Kimra, and Katsuji Nagaura. Piv observation of prewhirl flow upstream of a turbopump inducer. *Journal of Flow Visualization and Image Processing*, 17(1):85–98, 2010.
- [11] Yutaka Ito, Atsuhiko Tsunoda, Yuto Kurishita, Satoshi Kitano, and Takao Nagasaki. Experimental visualization of cryogenic backflow vortex cavitation with thermodynamic effects. *Journal of Propulsion and Power*, 32(1):71–82, 2016.
- [12] Nobuhiro Yamanishi, Shinji Fukao, Xiangyu Qiao, Chisachi Kato, and Yoshinobu Tsujimoto. LES Simulation of Backflow Vortex Structure at the Inlet of an Inducer. *Journal of Fluids Engineering*, 129(5):587–594, 09 2006.
- [13] C. Brennen and A.J. Acosta. The dynamic transfer function for a cavitating inducer. *Journal of Fluids Engineering, Transactions of the ASME*, 98(2):182–191, 1976.
- [14] Y. Tsujimoto, K. Kamijo, and C. E. Brennen. Unified treatment of flow instabilities of turbomachines. *Journal of Propulsion and Power*, 17:636–643, 2001.
- [15] Satoshi Kawasaki, Takashi Shimura, Masaharu Uchiumi, and Yuka Iga. One-dimensional analysis method for cavitation instabilities of a rotating machinery. *Journal of Fluids Engineering, Transactions of the ASME*, 140(2), 2018. 021113.
- [16] S. Watanabe and Y. Tsujimoto. Prediction of Cavitation Surge Onset Point by One-Dimensional Stability Analysis. *International Journal of Fluid Machinery and Systems*, 14(2):199–207, 2021.
- [17] S.L. Ng and C. Brennen. Experiments on the Dynamic Behavior of Cavitating Pumps. *Journal of Fluids Engineering, Transactions of the ASME*, 100(2):166–176, 1978.
- [18] C.E. Brennen, C. Meissner, E.Y. Lo, and G.S. Hoffman. Scale effects in the dynamic transfer functions for cavitating inducers. *Journal of Fluids Engineering, Transactions of the ASME*, 104(4):428–433, 1982.
- [19] T. Ashida, K. Yamamoto, K. Yonezawa, H. Horiguchi, Y. Kawata, and Y. Tsujimoto. Measurement of dynamic characteristics of an inducer in cavitating conditions. *International Journal of Fluid Machinery and Systems*, 10(3):307–317, 2017.
- [20] K. Yonezawa, J. Aono, D. Kang, H. Horiguchi, Y. Kawata, and Y. Tsujimoto. Numerical evaluation of dynamic transfer matrix and unsteady cavitation characteristics of an inducer. *International Journal of Fluid Machinery and Systems*, 5(3):126–133, 2012.
- [21] Sheldon Rubin. Longitudinal instability of liquid rockets due to propulsion feedback (POGO). *Journal of Spacecraft and Rockets*, 3(8):1188–1195, 1966.
- [22] Mitsuru Shimagaki, Toshiya Kimura, Tomoyuki Hashimoto, Mitsuo Watanabe, and Yoshiki Yoshida. Investigation of backflow structure in a turbopump inducer with the piv method. volume 5, pages 4877–4885, 2007.
- [23] Keita Yamamoto, Satoshi Ukai, Taro Fukuda, Satoshi Kawasaki, and Hideyo Negishi. Establishment of Prediction Model for Cavitation Surge Frequency and Onset in an Inducer Considering Dynamic Characteristics of Cavitation Compliance and Mass Flow Gain Factor. *Journal of Fluids Engineering*, 145(9):091501, 05 2023.
- [24] Sheldon Rubin. An Interpretation of Transfer Function Data for a Cavitating Pump. *40th AIAA/ASME/SAE/ASEE Joint Propulsion Conference and Exhibit*, 2004.